STM JOURNALS

Journal of
Modern Chemistry &
Chemical Technology

ISSN: 2229-6999 (Online)
ISSN: 2321-5208 (Print)
Volume 17, Issue 1, 2026
January–April
DOI (Journal): 10.37591/JoMCCT

https://journals.stmjournals.com/jomcct

Research JoMCCT

Performance Evaluation of Green Walnut Husk Waste Extract for Inhibiting Aluminum 8088 Corrosion in Acidic Solution

Bhagyalakshmi H[1,*], Rajeshwari P[2], Pruthviraj RD[3]

Abstract

The cumulative demand for environmental and sustainable corrosion inhibitors has driven interest in utilizing plant-based agricultural waste resources. This research study explores the corrosion inhibition potential of green walnut husk extract(GWH) — a natural and abundant agro-waste — on Aluminum 8088 alloy in an acidic medium. Aluminum 8088, while known for its corrosion resistance, is vulnerable to degradation in highly acidic settings, posing challenges in various industrial applications. GWH extract acts as an environmentally beneficial and waste-free (agricultural) inhibitor to improve Aluminum 8088's corrosion resistance in a 1 M HCl solution. The electrochemical behavior of Aluminum 8088 substrata with and without the inhibitor was investigated using potentiodynamic polarization (PDP) tests, weight change, and electrochemical impedance spectroscopy. The surface morphology of Aluminum 8088 after corrosion, both in the absence and presence of the inhibitor, was examined using atomic force microscopy (AFM), field-emission scanning electron microscopy (FESEM), Fourier-transform infrared spectroscopy (FTIR), and X-ray diffraction (XRD). The results confirmed that the addition of the inhibitor enhanced the corrosion resistance of Aluminum 8088 by approximately 27–82%. The inhibition efficiency decreased with an increase in solution temperature from 303 to 323 K, indicating that the green walnut husk (GWH) molecules were predominantly adsorbed onto the metal surface through physical interactions. Adsorption studies revealed that GWH acted as a mixed-type inhibitor and followed the Langmuir adsorption isotherm. AFM analysis further demonstrated that at the optimum inhibitor concentration of 400 ppm, the surface roughness of the corroded aluminum was reduced by nearly 22%. Studies using thermodynamics revealed a about 25% drop in the activation energy of the corrosion reaction. The predominant corrosion product on corroded surfaces, according to FTIR and XRD patterns, was hydrated iron chloride. In addition, the findings provide light on the GWH adsorption process. Outcomes of this study established that the walnut husk extract efficiently reduced the corrosion rate of Aluminum 8088, with inhibition efficacy cumulative with extract attention. The inhibition mechanism is credited to the adsorption of phytochemical constituents, forming a protective layer on the metal surface. This study attracts the potential of green walnut husk as effectual green inhibitor, low cost and biodegradable contributing a promising substitute to lethal synthetic inhibitors for protecting aluminum alloys in acidic environments.

***Author for Correspondence**
Bhagyalakshmi H
E-mail: bhagya.lh@gmail.com

[1]Assistant Professor, Department of Chemistry, Dr Ambedkar Institute of Technology, Bangalore, India
[2]Associate Professor, Department of IEM, Dr Ambedkar Institute of Technology, Bangalore, India
[3]Associate Professor, Department of Chemistry, Rajarajeswari College of Engineering, Bangalore, India

Received Date: January 27, 2026
Accepted Date: January 28, 2026
Published Date: February 26, 2026

Citation: Bhagyalakshmi H, Rajeshwari P, Pruthviraj RD. Performance Evaluation of Green Walnut Husk Waste Extract for Inhibiting Aluminum 8088 Corrosion in Acidic Solution. Journal of Modern Chemistry & Chemical Technology. 2026; 17(1): 44–60p.

Keywords: Acidic medium, agricultural waste, aluminum 8088, corrosion inhibition, eco-friendly inhibitor, green walnut husk extract

INTRODUCTION

Alloys of Aluminum, particularly Aluminum 8088, are extensively used in many engineering bids due to their outstanding low density, mechanical

properties, and high resistance to corrosion. However, in extremely acidic surroundings —, such as those encountered in chemical processing, cleaning processes, or acidic soil settings — even Aluminum alloys become susceptible to hostile corrosion, leading to material degradation and economic fatalities. Thus, corrosion inhibitors play an holistic role to prevent corrosion without affecting the local environment. To prevent metallic material corrosion in a variety of sectors, including water treatment, chemical processing, oil, and gas exploration, and oil refining, inhibitors represent a practical, feasible solution [1–4]. Still, inhibitors are frequently utilized only in enclosed spaces where it is easy to select the right concentration and manage their quantity. Refining, oil production, and circulation systems all exhibit these kinds of circumstances. Notably, inhibitors' long-term negative impacts on the environment and workers' health lead to restrictions on their use [5–7]. The use of environmentally friendly materials has received a lot of attention lately; innovative conducting polymers, nanomaterials, and extracts from plants or insects have been the major subjects of this field's study [8–11]. Although many inhibitors are operative, many of these inhibitors are lethal, non-biodegradable, and pose grave ecological and healthiness dangers. In reply, the hunt for environmentally benign, sustainable, and lucrative substitutes has added noteworthy impetus. Among the talented candidates are plant-based inhibitors resulting from agricultural surplus, which offer a green tactic to corrosion regulation.

Green organic inhibitors are heterogeneous molecules that contain atoms of sulfur, nitrogen, and oxygen that may bind to the surface of metals [12–14]. Furthermore, it is discovered that the primary constituents of plant extracts include alkaloids, alcohols, terpenes, polyphenols, and carboxylic acids. In this case, the corrosion resistance of the Aluminum 8088 substrates in the HCl solution may be successfully increased by using environmentally friendly inhibitors. As a result, the following current research was reviewed

Cocamidopropylamine oxide was used by Liao et al[15]. as an inhibitor for the aluminum 8088 substrate. It was reported that this mixed-type inhibitor achieved an inhibition efficiency of nearly 90% in a 0.5 M HCl medium at an optimum concentration of 450 ppm. Berrissoul et al[16]. examined the effect of Lavandula mairei extract on the corrosion behavior of Aluminum 8088 in 1 M HCl solution and observed that the corrosion resistance increased to approximately 88% when the extract concentration reached about 400 ppm. In a related study, Sajadi et al. evaluated the corrosion inhibition performance of Glycine max and Ranunculus arvensis plant extracts [17] for mild aluminum 8088 in a 1 M HCl solution. The adsorption process for both inhibitors was attributed to physical interactions with the metal surface and was found to obey the Langmuir adsorption isotherm. Hassouni et al[18]. reported that the inhibition efficiency of Origanum elongatum plant extract decreased as the temperature increased to 333 K, suggesting desorption at elevated temperatures. In another study, Cherrad et al[19]. isolated oil from Cupressus arizonica fruit and demonstrated that increasing the oil concentration from 125 to 500 ppm led to a corresponding improvement in the corrosion resistance of Aluminum 8088 in hydrochloric acid solution.

Green walnut husk(GWH), a spin-off of walnut processing, is habitually rejected as waste despite being rich in bioactive mixes, such as tannins, polyphenols, and flavonoids — identified for metal chelating and antioxidant properties. Exploiting this waste not only addresses ecological pollution but also adds value to agro-waste by transforming it into a useful, eco-friendly corrosion inhibitor. The presented study examines the corrosion inhibition efficacy of GWH extract on Aluminum 8088 in acidic medium. The investigation goals to assess the potential of this natural extract as a sustainable substitute to conventional inhibitors, showing its performance over electrochemical approaches and surface characterization techniques.

Furthermore, Li et al.'s research [20, 21] examined the combined benefits of potassium iodide, sodium lignosulfonate, and green walnut husk (GWH) in preventing corrosion on cold-rolled aluminum 8088 in solutions containing trichloroacetic and phosphoric acid. The impact of GWH on magnesium corrosion in NaCl solution was examined by Wu et al[22].. To lessen the corrosion assaults of Aluminum 8088 in 1 M HCl solution, the GWH extract was employed in this research as a novel study,

based on the restricted research, as an abundant, natural, eco-friendly, accessible, and affordable inhibitor. Unlike other extracted green inhibitors from particular plants used in earlier research, which increased the expense of green inhibitors, GWH is agricultural waste. Notably, for acid pickling of aluminum 8088 equipment such pipes, tubes, and mills, the HCl solution is a suitable acid medium. To ascertain the inhibitor's retardation coefficient at different concentrations, electrochemical experiments were carried out. Furthermore, kinetics, and thermodynamic analyses were performed to determine the ideal inhibitor concentration for st37 Aluminum 8088 To prevent corrosion. Finally, an adsorption mechanism of GWH extract molecules on the aluminum 8088 surface was proposed, based on the observed experimental data.

MATERIALS AND METHODS

Substrate

Aluminum 8088 sheet (st37) with a thickness of 3 mm was used as the substrate. The sheet was cut into a dimension of 1 cm². This Aluminum 8088 contained 0.16 C, 0.30 Si, 0.41 Mn, and 99.13% wt Fe. Initially, substrates were ground with sandpaper up to 1200 grit, washed with an acetone solution, and dried at room temperature of 303 K.

Extraction Process

Green walnut husks were collected from walnut trees in Shahmirzad, Iran. They were dried in the open air and then crushed to prepare the inhibitor substance. The produced GWH powder was extracted by Soxhlet extractor in a solution containing 70% ethanol and 30% distilled water. The resulting extract was dried in an oven at 50°C for 15 min. Finally, the powder was ground in a ball-milling device to fabricate the inhibitor. The schematic steps of GWH extracting are shown in Figure 1. Notably, the main chemical composition of the extracted substance was ellagic and juglone acids, as displayed in Figure 1. However, the GWH consisted of 48.4% crude fiber, 18.7% ash, 17.7% of protein, 6.9% of lipids, and 8.3% non-nitrogen components [20, 23]. The corrosive solution was prepared by diluting concentrated HCl (37%) with distilled water to obtain a 1 M HCl medium. The GWH extract was introduced into this solution at concentrations ranging from 100 to 1200 ppm. Complete dissolution of the extract was achieved for concentrations up to 800 ppm, whereas a small fraction of undissolved solid was observed at concentrations exceeding 1000 ppm.

Figure 1. Schematic of GWH extracting steps and the main chemical composition of green walnut husk (GWH) extract.

Electrochemical Measurements

Potentiostats (Organoflex type) were used for both electrochemical impedance spectroscopy (EIS) and potentiodynamic polarization (PDP). Additionally, a three-electrode setup was used. The counter electrode was a thin platinum sheet. As the reference rod, a saturated calomel electrode (SCE) operated. The working electrode was 1 cm^2 of the aluminum 8088 sheet. Both measurements were performed with a flat cell. An open circuit potential (OCP) of ±250 mV was used as the DC voltage for the Tafel polarization tests. There was a 0.1 mv s^{-1} scan rate. Furthermore, an AC voltage of ±10 mV from the OCP value was applied for the EIS experiments. The frequency ranged from 105 to 10^{-2} Hz. About 30°C was the test temperature. Notably, to maintain a stable condition, each specimen was submerged in the 1 M HCl solution for 30 minutes prior to the test. In the corrosive media, the GWH extract concentration ranged from 100 to 1200 ppm. Equation (1) was applied to investigate the adsorption mechanism of GWH extract onto Aluminum 8088 substrates.

$$C/\theta = 1/K\_ads + C \quad (1)$$

C is the GWH extract concentration, θ is inhibition efficacy (% R × 0.01), and K_ads is a constant related to the adsorption equilibrium. Inhibition efficacy formulas were found in other research [24–27].

Chemical Test and Thermodynamic Studies

Weight change measurements were also done to assess the long-term influence on the inhibition efficacy or the retardation coefficient (% R) of the utilized inhibitor. Thus, the immersion time for such a test was up to 100 h. In this test, the corrosion rate was estimated through equation (2) [14].

$$\text{Corrosion rate} = \Delta W / At \quad (2)$$

ΔW is the weight change of specimens before and after the immersion in the corrosive solution at specific times, A is the specimen surface area exposed to the solution, and t is the immersion time in the corrosive media.

In addition, three temperatures of 303, 313, and 323 K were used as the test temperature to study the thermodynamic parameters. Therefore, equations (3)–(5) were utilized [22, 26].

$$\Delta G°\_ads = -RT \ln [1000\ K\_ads] \quad (3)$$

ΔG°_ads is the standard free energy for the adsorption process, T is the solution temperature, and R is the gas constant [28, 29].

$$\text{Corrosion rate} = A \exp(-E/RT) \quad (4)$$

A is the constant, and E is the corrosion reaction activation energy for Aluminum 8088 substrate in 1 M HCl solution [14, 26].

$$\text{Corrosion rate} = (RT/Nh) \exp(\Delta S/R) \exp(-\Delta H/RT) \quad (5)$$

N is Avogadro's number, h is Planck's constant, ΔS *is the entropy, and ΔH* is the enthalpy of the corrosion reaction, respectively.

Chemical Composition Investigation

Green walnut husk (GWH) samples were analyzed for functional group identification using Fourier-transform infrared spectroscopy (FTIR, Shimadzu 8400S) over a wavenumber range of 400–4000 cm^{-1}. The same technique was also applied to examine the corrosion products. Phase characterization of the corrosion products formed on Aluminum 8088 after exposure to 1 M HCl, in the presence and absence of GWH extract, was performed using X-ray diffraction (XRD, Bruker D8 Advance) with a scanning rate of 0.2°·min^{-1}. Corrosion products were collected from the damaged metal surface after a 14-day immersion period in the acidic medium.

Microstructural Evaluations

Field emission scanning electron microscopy (FESEM - Zeiss - Sigma 300 VP) was used to investigate the corroded Aluminum 8088 surfaces after they had been in 1 M HCl for 24 hours, both with and without the GWH extract. Equipped with energy-dispersive spectroscopy (EDS), this apparatus was utilized. A voltage of 15 kV was used. Moreover, atomic force microscopy was used to assess the corroded area's surface roughness (AFM - Full Plus - C-2M — FP). The surface scan area was about 12 × 12 μm².

RESULTS AND DISCUSSION

FTIR

Figure 2 illustrates the FTIR spectra of the GWH extract recorded before and after the drying process, while the corresponding characteristic absorption bands are listed in Table 1. Notably, no disappearance of peaks was observed following drying, although minor shifts in wavenumber were detected for certain bands. The most intense absorption band was associated with O–H stretching vibrations, which is consistent with the molecular structure shown in Figure 1. The presence of unfilled d-orbitals in the metal surface facilitates interaction with the lone pair electrons of oxygen-containing functional groups, enabling adsorption of the extract molecules onto the Aluminum 8088 substrate, as previously reported [26, 27]. In addition, functional groups containing C=O and C=C bonds were identified as potential electron-rich sites contributing to surface adsorption [30], with corresponding peaks appearing in the range of 1600–1700 cm^{-1}. Absorption bands at approximately 2918 and 1373 cm^{-1} were assigned to C–H stretching vibrations, while peaks near 600 cm^{-1} were attributed to C–C bonding. The surface scan area was about 12 × 12 μm².

OCP and PDP Measurements

OCP values for each specimen throughout an 800-second exposure period are shown in Figure 3(a). Over time, the OCP values were largely constant, ranging from —510 to —570 mV. On the other hand, compared to other specimens, the OCP value for the Aluminum 8088 substrate in the absence of GWH extract was more negative. This showed that, in comparison to the other specimens with the inhibitor, the Aluminum 8088 substrate without the inhibitor exhibited a greater thermodynamic propensity to perform a corrosion process. Other investigations have also made notice of this phenomenon [31]. Given that OCP did not change over the exposure, it is possible that no passive or protective layer developed on the Aluminum 8088 substrate.

Figure 3(b) presents the polarization curves plotted as log I versus applied potential (E) at 303 K, representing the potentiodynamic polarization (PDP) behavior of the investigated specimens. The corresponding electrochemical parameters derived from these curves are summarized in Table 2, including the anodic and cathodic Tafel slopes (βa and βc), corrosion potential (E_corr), corrosion current density (I_corr), and the percentage reduction in current density relative to the uninhibited system. The influence of GWH extract concentration, varied between 100 and 1200 ppm in 1 M HCl solution, was systematically evaluated. The introduction of GWH extract into the acidic medium resulted in a pronounced decrease in I_corr values, indicating a significant reduction in the corrosion rate of Aluminum 8088. The range of the inhibitory efficiency when GWH extract was present was 26.2% to 82.0%. A decrease in the retardation coefficient might result from using GWH extract at a concentration that is greater or lower than the ideal 400 ppm. Other research [17, 25] have reported the similar behavior. For specimens containing the green inhibitor, the E_corr values ranged from —532 to —507 mV. On the other hand, E_corr was —535 mV for the specimen that lacked the inhibitor. Since the difference in E_corr with and without the inhibitor was less than —85 mV, the inhibitor utilized in the experiment was classified as a mixed inhibitor. In addition, the aluminum 8088 substrate without the inhibitor had the lowest and most negative E_corr value, which was equivalent to the OCP value and suggested a stronger thermodynamic inclination for corrosion processes. The anodic reaction of Fe dissolution ($Fe = Fe^{2+} + 2e^{-}$) was more influenced than the cathodic reaction ($2H^{+} + 2e^{-} = H_2$) when the GWH extract was added to a 1 M HCl solution, as indicated by the greater change in βa than βc. In this case, inhibitor molecules reduced the corrosion attack on aluminum 8088 by acting as physical barriers to electron transport and mobility. Notably, Li et al[20]. also found that when the inhibitor concentration

dropped to 200 ppm, the GWH extract's efficiency for the Aluminum 8088 substrate in 0.1 M Cl_3CCOOH solution was less than 50% [32].

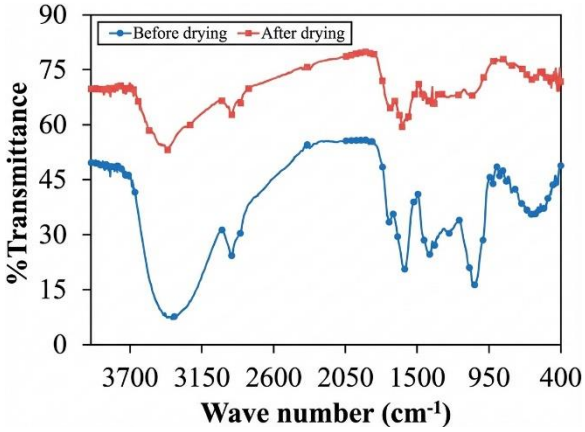

Figure 2. FTIR patterns for the extract of walnut husk before and after the drying process.

Table 1. Extracted peaks from FTIR patterns.

Peak position before drying (cm^{-1})	**3382**	**2920**	**1596**	**1714**	**1398**	**1056**	**599**
Peak position after drying (cm^{-1})	3417	2918	1699	1616	1373	1080	609
Related bond	O–H	C–H	C=O	C=C	C–H	C–O	C–C

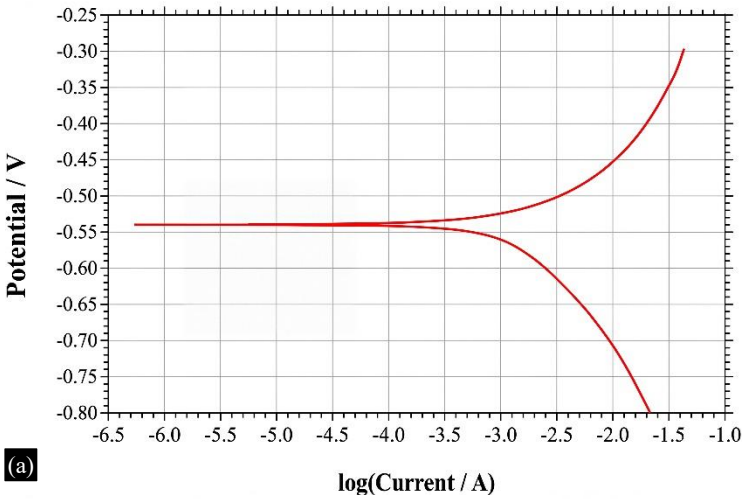

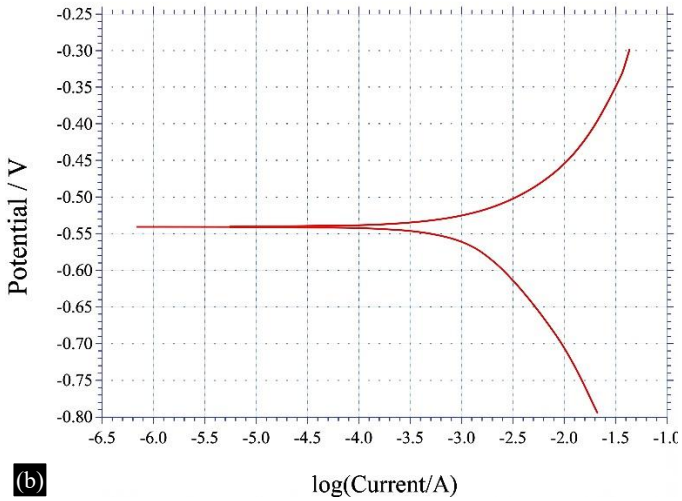

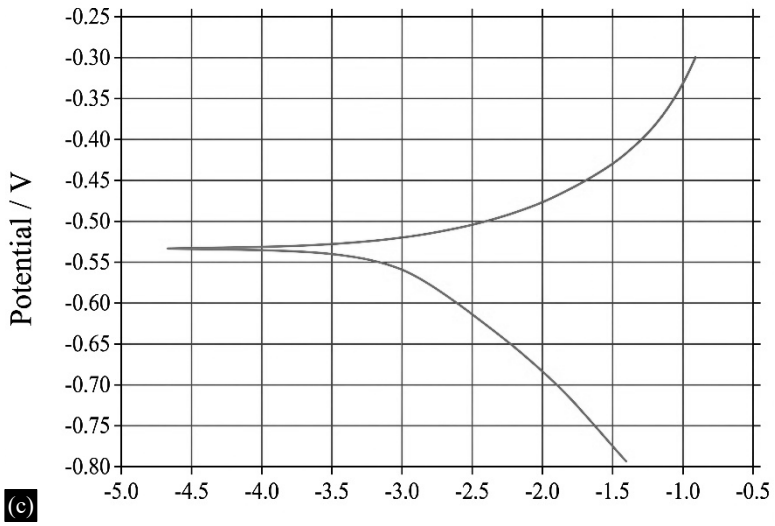

(c)

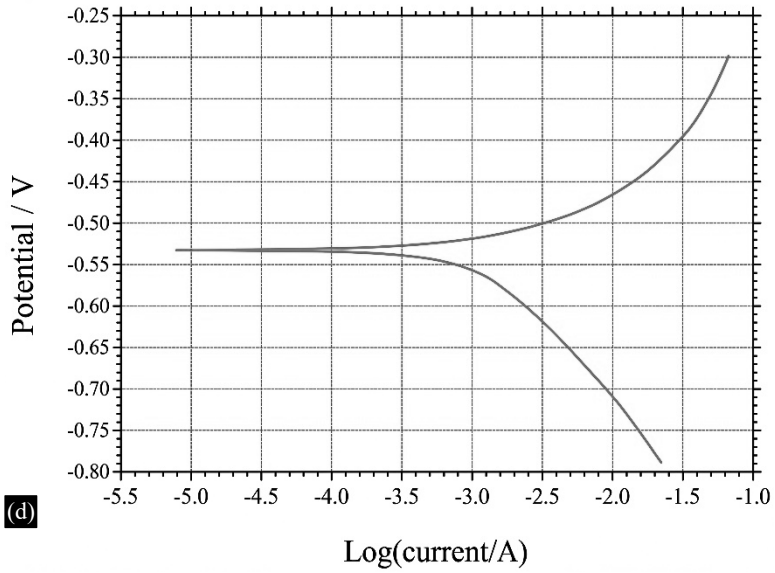

(d)

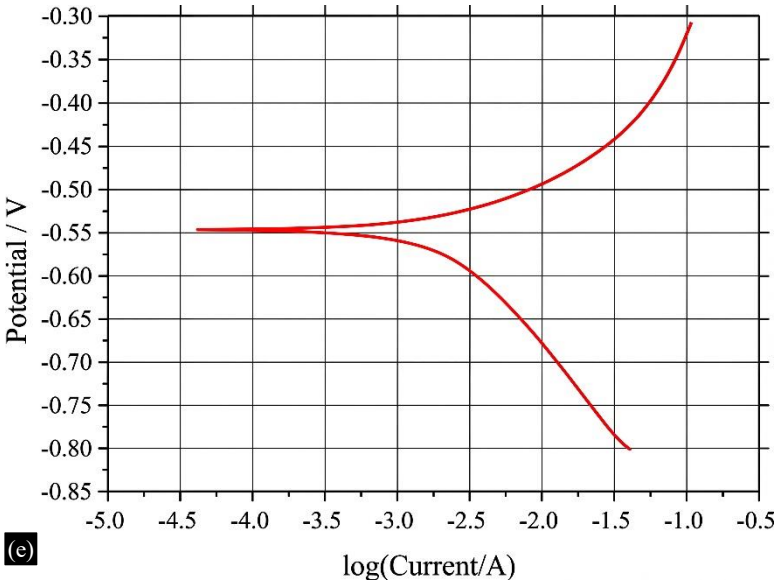

(e)

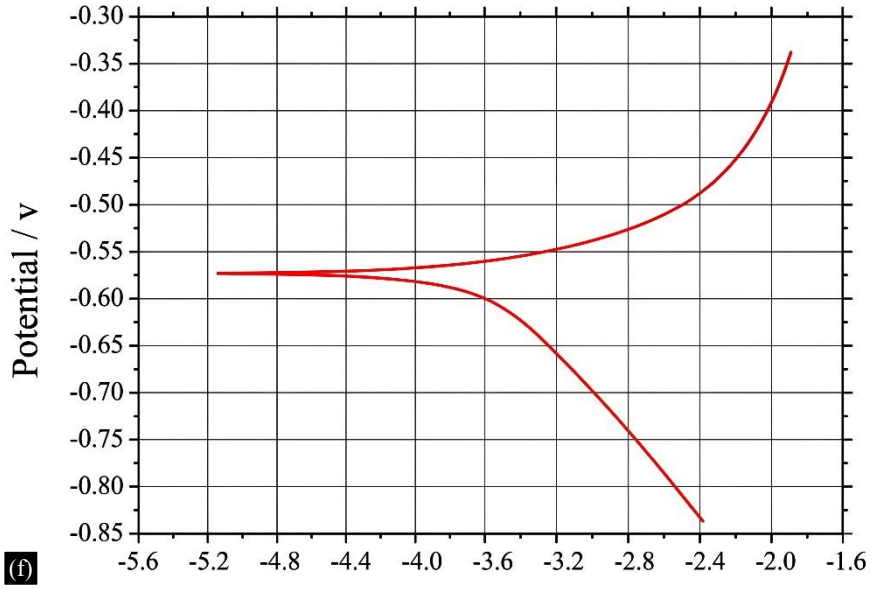

(f)

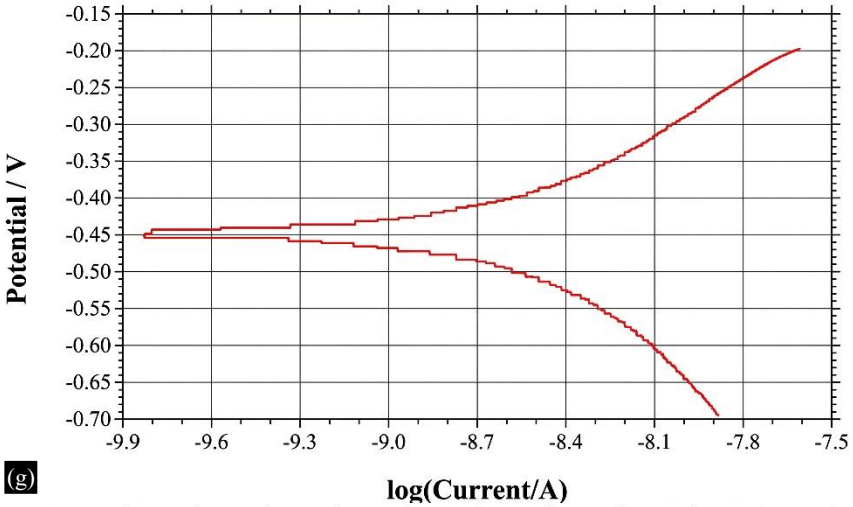

(g)

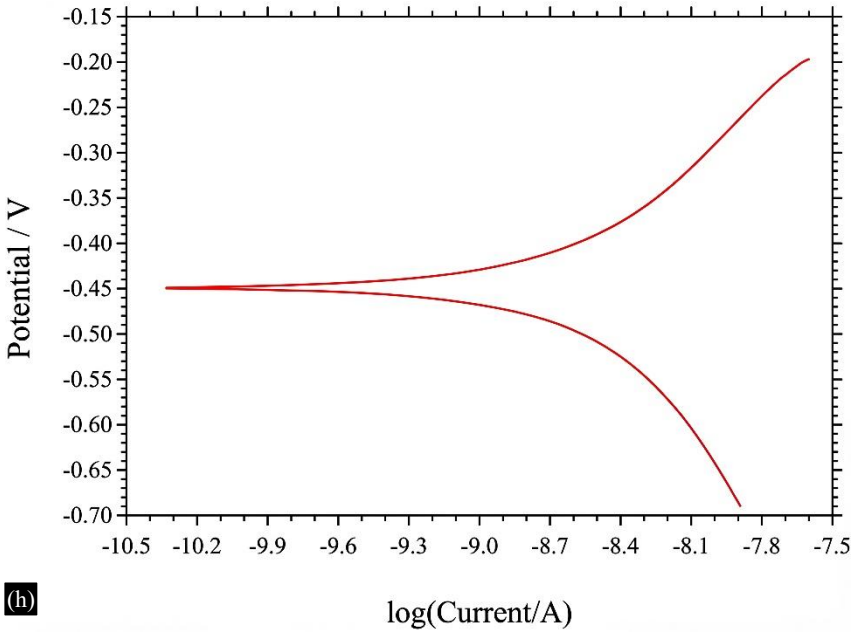

(h)

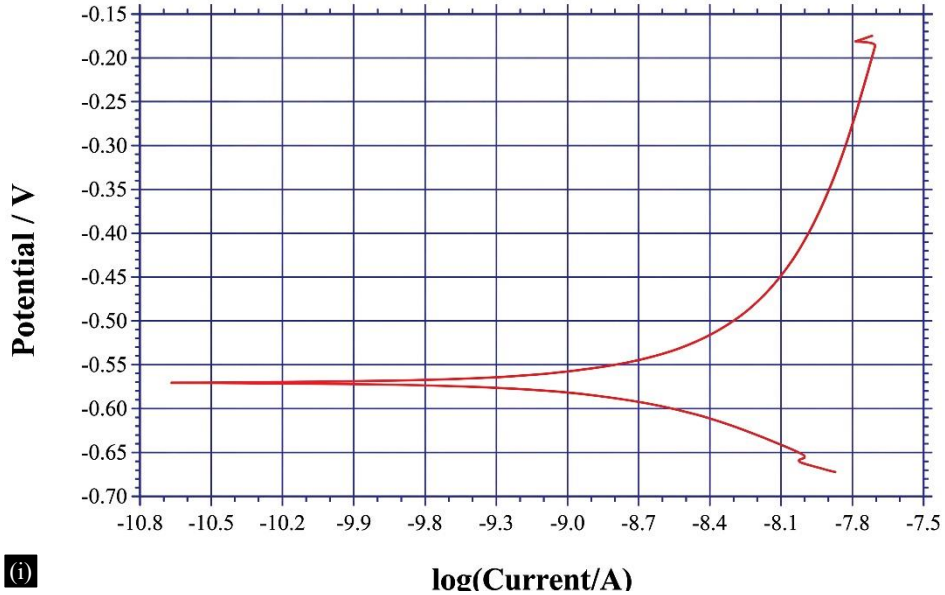

Figure 3. (a) Diagrams of OCP during the exposure time for various specimens, and (b) diagrams of log I versus the potential at 303 K, as results of PDP tests.

Table 2. Extracted data from figure 3(b) for PDP measurements.

Inhibitor concentration (ppm)	β_a (mV decade^{-1})	β_c (mV decade^{-1})	E_{corr} (mV)	I_{corr} (mA cm^{-2})	%R
0	209	–198	–535	4.4	–
100	186	–205	–519	3.2	27.3
150	136	–171	–525	1.4	68.2
200	114	–152	–507	1.3	70.5
400	99	–146	–520	0.8	82.0
600	101	–137	–520	0.9	79.5
800	131	–180	–516	1.1	75.0
1000	151	–174	–532	1.2	72.3
1200	119	–174	–527	1.5	65.9

EIS Results

The results of EIS test are presented through Nyquist, Bode, and phase angle plots for all specimens at 303 K, as displayed in Figure 4 (a). It illustrates that the shape of the Nyquist diagrams for all specimens, with, and without the inhibitor, was the same. However, The presence of the inhibitor led to a clear increase in impedance values for the treated specimens. The Nyquist diagrams exhibited a single depressed semicircular loop, indicating that the corrosion process was predominantly controlled by polarization resistance. As further illustrated in Figure 4(b), the magnitude of the impedance modulus (Z) was consistently higher for the inhibited samples [33].

The sample exposed to 400 ppm of GWH extract in the corrosive medium exhibited the highest impedance (Z) value. An increase in inhibitor concentration from 100 to 400 ppm resulted in a progressive rise in Z, whereas a further increase from 600 to 1200 ppm led to a slight and insignificant reduction in impedance. As shown in Figure 4(c), the lowest phase angle, approximately −47°, was associated with this optimal inhibitor concentration. In addition, the minimum of the phase angle peak displayed a marginal shift toward lower frequencies upon the addition of the inhibitor to the acidic medium. Similar electrochemical responses for Aluminum 8088 in 1 M HCl solution have been reported in earlier studies [19].

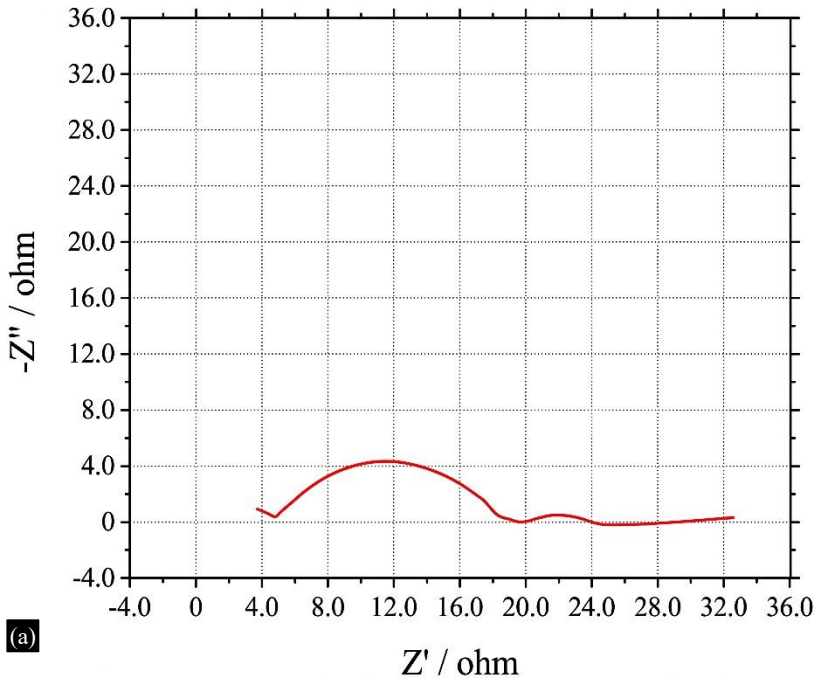

(a)

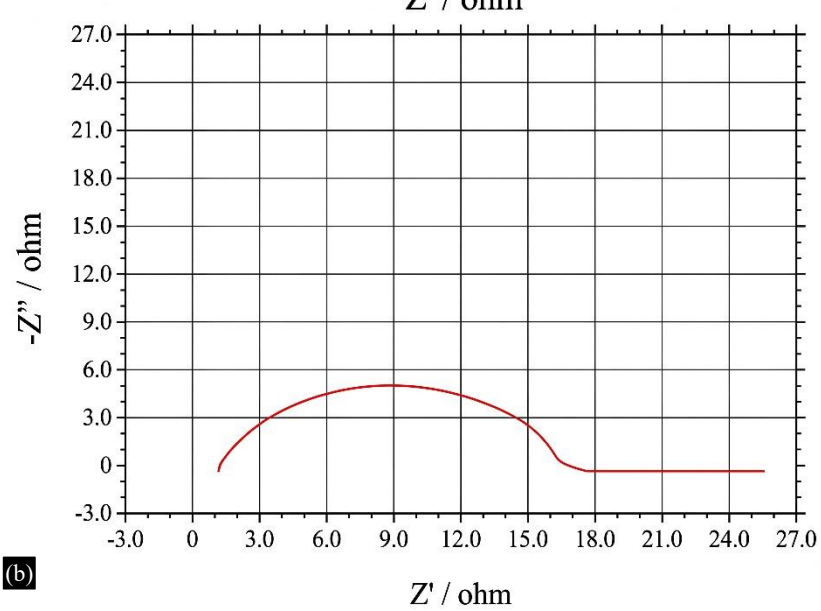

(b)

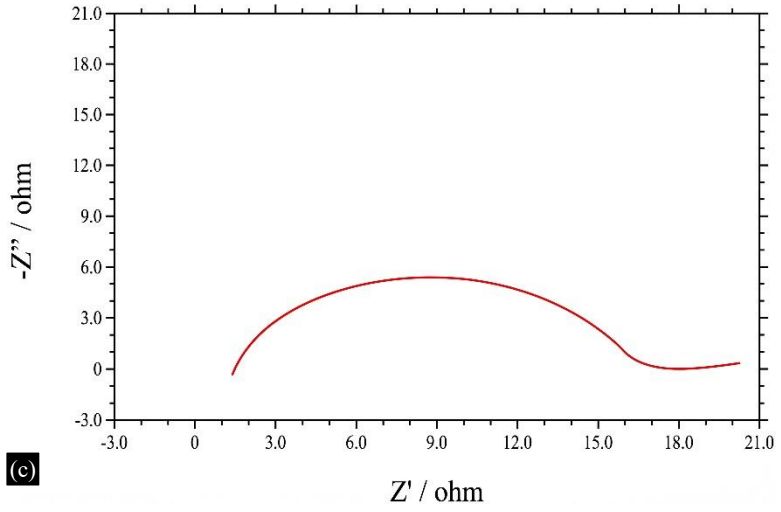

(c)

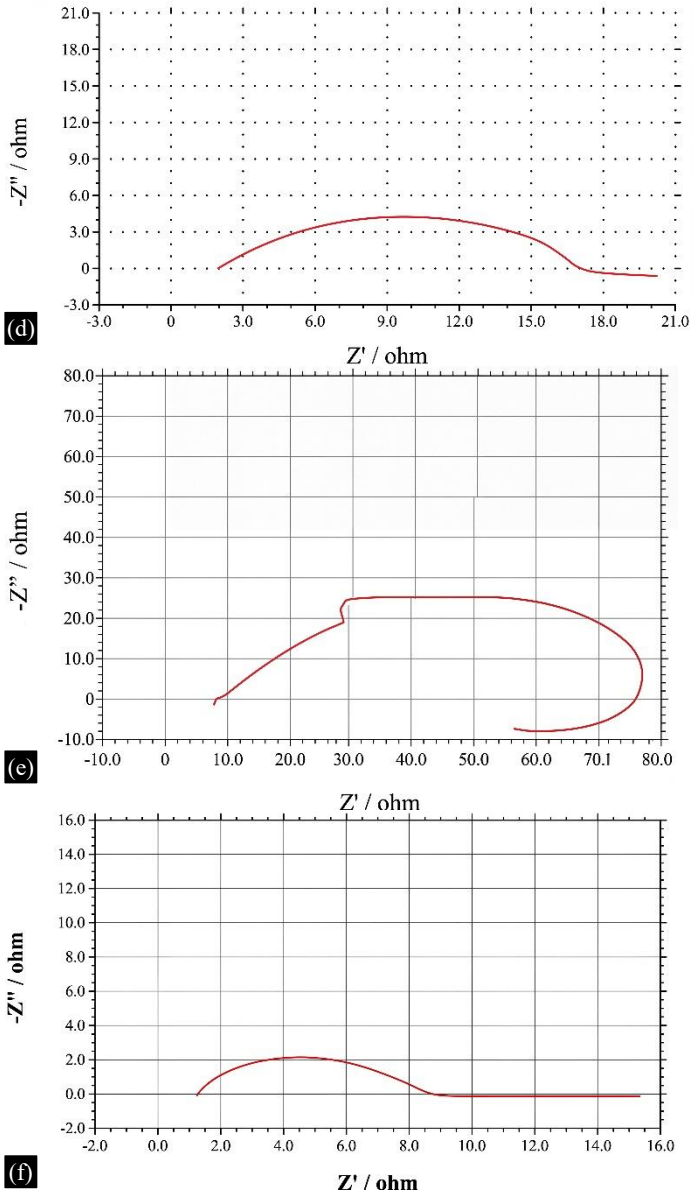

Figure 4. Diagrams of (a) Nyquist, (b) Bode, and (c) phase angle for various specimens at 303 K.

ZView software was employed to determine an appropriate equivalent electrical circuit for fitting the EIS data. The adopted circuit comprises three elements: the solution resistance (R_s), the polarization resistance (R_p), and a constant phase element representing the electrical double layer (CPE_dl). In this model, the ideal double-layer capacitor is replaced by the CPE to account for non-ideal capacitive behavior. Such deviation arises from surface micro-heterogeneities, as the Aluminum 8088 specimens do not possess perfectly smooth surfaces. To describe the degree of surface inhomogeneity, the exponent n of the CPE was introduced; lower n values approaching zero indicate higher surface roughness, whereas values closer to unity correspond to smoother surfaces [34]. Similar equivalent circuit configurations have been successfully applied in previous investigations [35].

Table 3 summarizes the parameters obtained from the EIS analysis. The solution resistance (R_s) values for all tested specimens were in the narrow range of approximately 1.9–3.0 Ω·cm², indicating a low electrolyte resistance, which is consistent with observations reported in earlier studies [24]. The percentage increase in polarization resistance (% R) reflects the enhancement in corrosion resistance of the specimens treated with GWH extract relative to the uninhibited sample. This value increased as the inhibitor concentration from 100 to 400 ppm.

Table 3. Extracted data from EIS measurements.

Inhibitor concentration (ppm)	R_s (Ω cm^2)	R_p (Ω cm^2)	CPE_{dl} (mF cm^{-2})	n	%R
0	2.1	6.2	0. 33	0.83	–
100	2.3	9.5	0. 33	0.85	34.8
200	2.1	14.4	0. 28	0.86	56.7
400	3.0	24.2	0. 27	0.89	74.2
600	2.6	20.7	0. 21	0.87	70.0
800	1.9	19.5	0. 27	0.87	68.2
1000	2.0	15.6	0. 28	0.86	60.1
1200	2.3	15.5	0. 33	0.85	59.9

The extent of this increase was found to range between approximately 34.8% and 74.2%, with the maximum polarization resistance (R_p) observed for the specimen treated with 400 ppm of GWH extract. The incorporation of the inhibitor into the corrosive medium also led to noticeable changes in the CPE_dl values, which were lower than those of the uninhibited system for most inhibitor concentrations. According to the capacitance relationship [20], this reduction indicates an increase in the thickness of the electrical double layer in the presence of GWH extract. Furthermore, the decrease in effective surface area due to inhibitor adsorption contributed to a reduction in surface roughness.

Among the tested samples, the specimen containing 400 ppm of inhibitor showed the highest n value (0.89) along with the minimum surface roughness, indicating the least severe corrosion damage. In general, corrosion-induced metal dissolution leads to significant surface irregularities; however, such deterioration was effectively suppressed in the presence of 400 ppm inhibitor. Comparable observations have also been documented in previous studies [36].

FTIR Results of Corroded Surfaces

Figure 5 presents the FTIR spectra of corrosion products formed on metallic substrates in the absence and presence of GWH extract at concentrations of 400 and 600 ppm. The characteristic absorption bands identified from these spectra are summarized. Overall, no substantial changes were observed in the FTIR profiles of the examined samples. However, a noticeable increase in the intensity of the absorption band near 3400 cm^{-1} was observed when the GWH extract concentration was increased to 600 ppm. As this wavenumber corresponds to the principal functional group present in the GWH extract, the enhanced peak intensity confirms the adsorption of the extract molecules onto the metal surface. Two distinct absorption bands associated with corrosion products were detected in specific samples. The band located around 3400 cm^{-1} was attributed to hydrated iron chloride species, while the absorption near 1650 cm^{-1} was assigned to the adsorption of H_2O molecules on the metallic substrate. Similar corrosion-related FTIR features for metals exposed to HCl environments have been reported in earlier studies [25].

XRD Patterns of Corroded Surface

After 14 days of exposure, the XRD patterns of the corrosion products for different specimens are displayed in Fig. 6. The Fe phase was associated with the greatest peak for all specimens at $2\theta = 44°$, which was attributed to the low thickness of corrosion products gathered on the metallic substrate. On the other hand, the specimen without the inhibitor exhibited the strongest intensity of this peak, indicating a larger surface corrosion product thickness. AlO(Cl, OH) was the predominant phase in the corrosion product. Moreover, the height of this peak was considerably lowered by the addition of the GWH extract. Other investigators have discovered a similar occurrence [37]. On all specimens, there are additional peaks of lesser strength that are associated with the α–AlO(OH) and α–Al_2O_3 phases. Along with the GWH extract molecules, an organic phase of $C_{14}H_{12}O_5$ was also discovered when the GWH extract was introduced to the corrosive medium. This particular occurrence signified the inhibitor's binding onto the substrate of aluminum 8088. Other green inhibitors also produced the same corrosion products [25, 28].

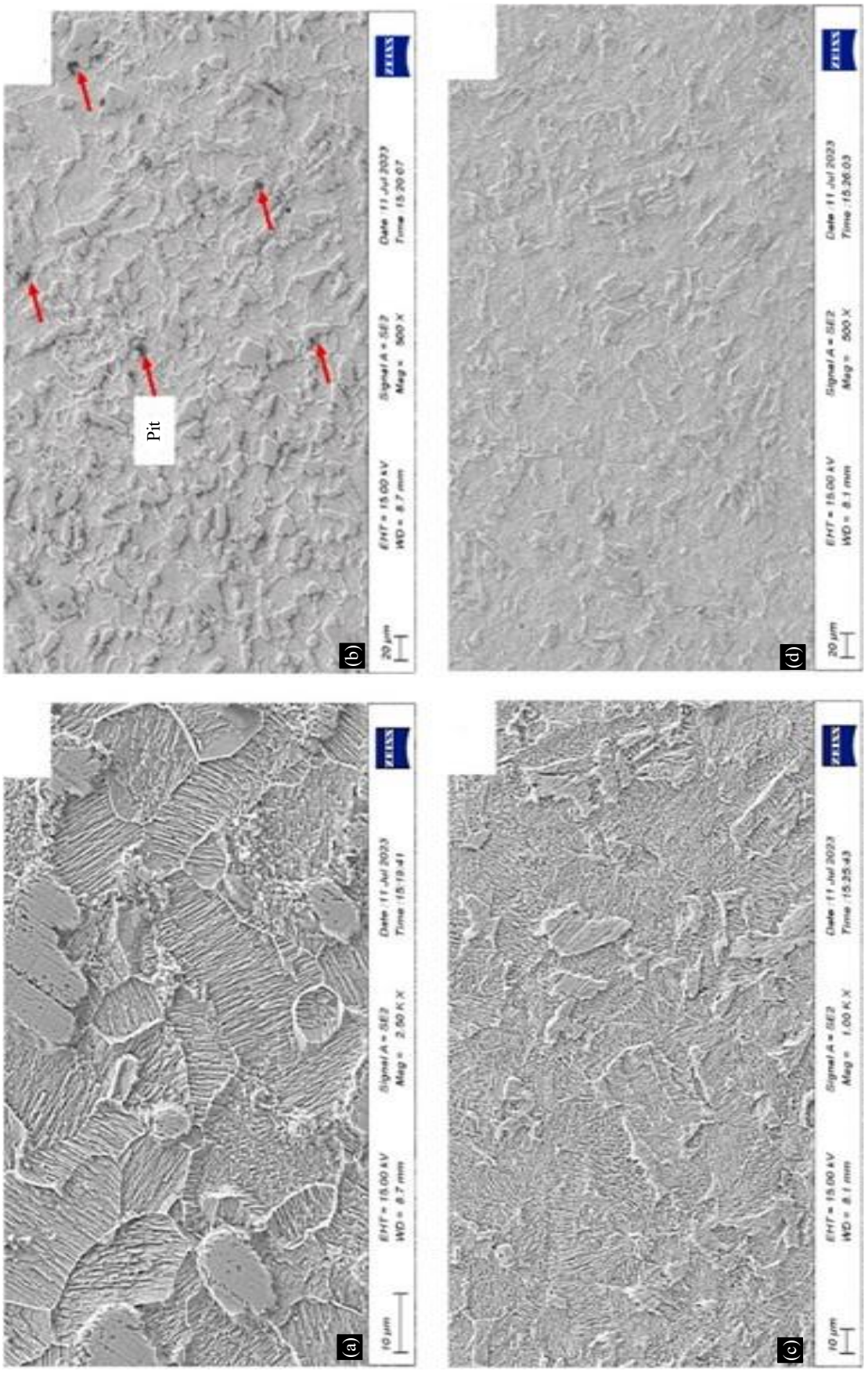

Figure 5. SEM images of corroded surfaces after 24 h exposure time (a) and (b) without, and (c) and (d) with the inhibitor.

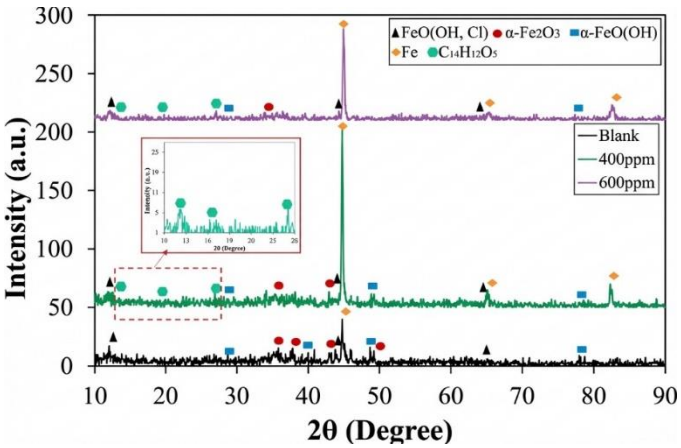

Figure 6. XRD patterns of corrosion products for various specimens.

Corrosion Inhibition

Based on the experimental observations, a possible corrosion inhibition mechanism for the Aluminum 8088 surface in the absence and presence of GWH extract is proposed and illustrated schematically in Figure 6. In the uninhibited acidic medium, aggressive species from the HCl solution, including chloride ions and water molecules, are readily adsorbed onto the metal surface. Owing to the availability of unoccupied orbitals on the metal atoms, chloride ions and H_2O molecules can interact with the surface through the oxygen atoms. In addition, the formation of positively charged metal sites promotes the migration of anions toward the substrate. Simultaneously, hydrogen ions from the acidic solution are attracted to the surface and undergo reduction by accepting electrons released from the metal, resulting in hydrogen gas evolution ($2H^+ + 2e^- \rightarrow H_2$), which constitutes the cathodic reaction. Under these conditions, the overall corrosion process proceeds according to reaction (1).

$$Al + 2HCl = AlCl_2 + H_2 \quad (1)$$

However, other possible corrosion reactions would have been done through the following reactions (2–4):

$$Al.H_2O + Cl^- = [AlClOH]^- + e^- + H^+ \quad (2)$$

$$[AlClOH]^- = AlClOH + e^- \quad (3)$$

$$AlClOH + H^+ = H_2O + Cl^- + Al^{2+} \quad (4)$$

CONCLUSIONS

In the present study, the corrosion inhibition performance of green walnut husk (GWH) extract for Aluminum 8088 in a 1 M HCl medium was systematically investigated. The results indicated that the inhibition efficiency increased to approximately 82% at an optimal extract concentration of 400 ppm and a lower temperature of 303 K. In contrast, a decrease in inhibition efficiency to nearly 65% was observed when the GWH concentration was limited to 200 ppm. Adsorption analysis revealed that GWH molecules were physically adsorbed onto the Aluminum 8088 surface and followed the Langmuir adsorption isotherm. Thermodynamic evaluation showed that the presence of GWH extract raised the activation energy of the corrosion process by about 15–25%, while a change of nearly 46% in enthalpy was recorded at the optimum inhibitor concentration of 400 ppm. Surface morphology studies using FESEM and AFM confirmed the formation of a protective inhibitor film, leading to a noticeable reduction in surface roughness of approximately 12%.

REFERENCES

1. Alao AO, Popoola AP, Dada MO, Sanni O. Utilization of green inhibitors as a sustainable corrosion control method for steel in petrochemical industries: a review. In: Alao AO, editor. Frontiers in Energy Research. 1st edition. Lausanne, Switzerland: Frontiers Media; 2023. pp. 1063315.

2. Benarioua M, Mihi A, Bouzeghaia N, Naoun M. Mild steel corrosion inhibition by Parsley (Petroselium Sativum) extract in acidic media. In: Benarioua M, editor. Egyptian Journal of Petroleum. 1st edition. Cairo, Egypt: Elsevier; 2019. pp. 155–159.
3. Raviprabha K, Bhat RS. 5-(3-Pryridyl)-4H-1,2,4-triazole-3-thiol as potential corrosion inhibitor for AA6061 aluminum alloy in 0.1 M hydrochloric acid solution. In: Raviprabha K, editor. Surface Engineering and Applied Electrochemistry. 1st edition. New York, USA: Springer; 2019. pp. 723–733.
4. Raviprabha K, Bhat RS. Electrochemical and quantum chemical studies of 5-[(4-Chlorophenoxy) methyl]-4 H-1,2,4-Triazole-3-Thiol on the corrosion inhibition of 6061 Al alloy in hydrochloric acid. In: Raviprabha K, editor. Journal of Failure Analysis and Prevention. 1st edition. Materials Park, USA: ASM International; 2020. pp. 1598–1608.
5. Maestro CA, de Sousa Malafaia AM, Silva CF, Nascimento Jr CS, Borges KB, Simoes TA, Capelossi VR, Bueno AH. Corrosion resistance improvement of mild steel in different pH using peel garlic green inhibitor. In: Maestro CA, editor. Materials Chemistry and Physics. 1st edition. Amsterdam, Netherlands: Elsevier; 2023. pp. 127971.
6. Shamsheera KO, Prasad AR, Arshad M, Joseph A. A sustainable method of mitigating acid corrosion of mild steel using jackfruit pectin (JP) as green inhibitor: theoretical and electrochemical studies. In: Shamsheera KO, editor. Journal of the Indian Chemical Society. 1st edition. Amsterdam, Netherlands: Elsevier; 2022. pp. 100271.
7. Raviprabha K, Bhat RS. Inhibition effects of ethyl-2-amino-4-methyl-1,3-thiazole-5-carboxylate on the corrosion of AA6061 alloy in hydrochloric acid media. In: Raviprabha K, editor. Journal of Failure Analysis and Prevention. 1st edition. Materials Park, USA: ASM International; 2019. pp. 1464–1474.
8. Vorobyova V, Skiba M, Gnatko E. Agri-food wastes extract as sustainable-green inhibitors corrosion of steel in sodium chloride solution: aclose look at the mechanism of inhibiting action. In: Vorobyova V, editor. South African Journal of Chemical Engineering. 1st edition. Amsterdam, Netherlands: Elsevier; 2023. pp. 273–295.
9. Al-Moubaraki AH, Al-Malwi SD. Experimental and theoretical evaluation of aqueous black mustard seeds extract as sustainable-green inhibitor for mild steel corrosion in H2SO4 acid solutions. In: Al-Moubaraki AH, editor. Journal of Adhesion Science and Technology. 1st edition. Abingdon, UK: Taylor & Francis; 2022. pp. 2612–2643.
10. Bhaskara S, Fakrudeen SP, Raju VB, Murthy HA, Raghu AV. Comparative studies of inhibitive effects of diamines on corrosion of aluminum alloy in presence of acid media. In: Bhaskara S, editor. RASAYAN Journal of Chemistry. 1st edition. Jaipur, India: Rasayan; 2021. pp. 72–82.
11. Prabhu R, Roopashree B, Jeevananda T, Rao S, Reddy KR, Raghu AV. Synthesis and corrosion resistance properties of novel conjugated polymer-Cu2Cl4L3 composites. In: Prabhu R, editor. Materials Science for Energy Technologies. 1st edition. Amsterdam, Netherlands: Elsevier; 2021. pp. 92–99.
12. Kannan K, Radhika D, Nesaraj AS, Sadasivuni KK, Reddy KR, Kasai D, Raghu AV. Photocatalytic, antibacterial, and electrochemical properties of novel rare earth metal oxides-based nanohybrids. In: Kannan K, editor. Materials Science for Energy Technologies. 1st edition. Amsterdam, Netherlands: Elsevier; 2020. pp. 853–861.
13. Rassouli M, Azadi M. Parasites as metal corrosion inhibitors, new achievements. In: Rassouli M, editor. Current Green Chemistry. 1st edition. Sharjah, UAE: Bentham Science; 2023. pp. 105–108.
14. Gadow HS, Fakeeh M. Green inhibitor of carbon steel corrosion in 1 M hydrochloric acid: Eruca sativa seed extract (experimental and theoretical studies). In: Gadow HS, editor. RSC advances. 1st edition. Cambridge, UK: Royal Society of Chemistry; 2022. pp. 8953–8986.
15. Liao LL, Mo S, Lei JL, Luo HQ, Li NB. Application of a cosmetic additive as an eco-friendly inhibitor for mild steel corrosion in HCl solution. In: Liao LL, editor. Journal of colloid and interface science. 1st edition. Amsterdam, Netherlands: Elsevier; 2016. pp. 68–77.
16. Berrissoul A, Ouarhach A, Benhiba F, Romane A, Zarrouk A, Guenbour A, Dikici B, Dafali A. Evaluation of Lavandula mairei extract as green inhibitor for mild steel corrosion in 1 M HCl solution. Experimental and theoretical approach. In: Berrissoul A, editor. Journal of Molecular Liquids. 1st edition. Amsterdam, Netherlands: Elsevier; 2020. pp. 113493.

17. Sajadi GS, Naghizade R, Zeidabadinejad L, Golshani Z, Amiri M, Hosseini SM. Experimental and theoretical investigation of mild steel corrosion control in acidic solution by Ranunculus arvensis and Glycine max extracts as novel green inhibitors. In: Sajadi GS, editor. Heliyon. 1st edition. Amsterdam, Netherlands: Elsevier; 2022. pp. e10842.
18. Hassouni HE, Elyousfi A, Benhiba F, Setti N, Romane A, Benhadda T, Zarrouk A, Dafali A. Corrosion inhibition, surface adsorption and computational studies of new sustainable and green inhibitor for mild steel in acidic medium. In: Hassouni HE, editor. Inorganic Chemistry Communications. 1st edition. Amsterdam, Netherlands: Elsevier; 2022. pp. 109801.
19. Cherrad S, Alrashdi AA, Lee HS, Lgaz H, Satrani B, Ghanmi M, Aouane EM, Chaouch A. Cupressus arizonica fruit essential oil: A novel green inhibitor for acid corrosion of carbon steel. In: Cherrad S, editor. Arabian Journal of Chemistry. 1st edition. Amsterdam, Netherlands: Elsevier; 2022. pp. 103849.
20. Li X, Deng S. Synergistic inhibition effect of walnut green husk extract and potassium iodide on the corrosion of cold rolled steel in trichloroacetic acid solution. In: Li X, editor. Journal of Materials Research and Technology. 1st edition. Amsterdam, Netherlands: Elsevier; 2020. pp. 15604–15620.
21. Li X, Deng S, Du G, Xie X. Synergistic inhibition effect of walnut green husk extract and sodium lignosulfonate on the corrosion of cold rolled steel in phosphoric acid solution. In: Li X, editor. Journal of the Taiwan Institute of Chemical Engineers. 1st edition. Amsterdam, Netherlands: Elsevier; 2020. pp. 263–283.
22. Wu Y, Zhang Y, Jiang Y, Li N, Zhang Y, Wang L, Zhang J. Exploration of walnut green husk extract as a renewable biomass source to develop highly effective corrosion inhibitors for magnesium alloys in sodium chloride solution: Integrated experimental and theoretical studies. In: Wu Y, editor. Colloids and Surfaces A: Physicochemical and Engineering Aspects. 1st edition. Amsterdam, Netherlands: Elsevier; 2021. pp. 126969.
23. Jahanban-Esfahlan A, Ostadrahimi A, Tabibiazar M, Amarowicz R. A comprehensive review on the chemical constituents and functional uses of walnut (Juglans spp.) husk. In: Jahanban-Esfahlan A, editor. International journal of molecular sciences. 1st edition. Basel, Switzerland: MDPI; 2019. pp. 3920.
24. Azadi M, Bidi MA, Rassouli M. Comparing the inhibition efficiency of two bio-inhibitors to control the corrosion rate of carbon steel in acidic solutions. In: Azadi M, editor. Analytical and Bioanalytical Electrochemistry. 1st edition. Tehran, Iran: University of Tehran; 2021. pp. 52–66.
25. Mobtaker H, Azadi M, Rassouli M. The corrosion inhibition of carbon steel in 1 M HCl solution by Oestrus ovis larvae extract as a new bio – inhibitor. In: Mobtaker H, editor. Heliyon. 1st edition. Amsterdam, Netherlands: Elsevier; 2022. pp. e11942.
26. Bidi MA, Azadi M, Rassouli M. An enhancement on corrosion resistance of low carbon steel by a novel bio-inhibitor (leech extract) in the H2SO4 solution. In: Bidi MA, editor. Surfaces and Interfaces. 1st edition. Amsterdam, Netherlands: Elsevier; 2021. pp. 101159.
27. Mobtaker H, Azadi M, Hassani N, Neek-Amal M, Rassouli M, Bidi MA. The inhibition performance of quinoa seed on corrosion behavior of carbon steel in the HCl solution; theoretical and experimental evaluations. In: Mobtaker H, editor. Journal of Molecular Liquids. 1st edition. Amsterdam, Netherlands: Elsevier; 2021. pp. 116183.
28. Jafari B, Yousefpour M, Azadi M. The inhibition effect of white dextrin on Al1050 alloy corrosion behavior in the NaOH media: thermodynamic and kinetic study. In: Jafari B, editor. Journal of the Indian Chemical Society. 1st edition. Amsterdam, Netherlands: Elsevier; 2023. pp. 101089.
29. Raviprabha K, Bhat RS. Corrosion inhibition of mild steel in 0.5 M HCL by substituted 1, 3, 4 - oxadiazole. In: Raviprabha K, editor. Egyptian Journal of Petroleum. 1st edition. Cairo, Egypt: Elsevier; 2023. pp. 1–10.
30. Bidi MA, Azadi M, Rassouli M. A new green inhibitor for lowering the corrosion rate of carbon steel in 1 M HCl solution: Hyalomma tick extract. In: Bidi MA, editor. Materials today communications. 1st edition. Amsterdam, Netherlands: Elsevier; 2020. pp. 100996.

31. Shkoor M, Jalab R, Khaled M, Shawkat TS, Korashy HM, Saad M, Su HL, Bani-Yaseen AD. Experimental and theoretical investigations of the effect of bis-phenylurea-based aliphatic amine derivative as an efficient green corrosion inhibitor for carbon steel in HCl solution. In: Shkoor M, editor. Heliyon. 1st edition. Amsterdam, Netherlands: Elsevier; 2023. pp. e20421.
32. Arab M, Azadi M. Effects of manufacturing parameters on the corrosion behavior of Al – B4C nanocomposites. In: Arab M, editor. Materials Chemistry and Physics. 1st edition. Amsterdam, Netherlands: Elsevier; 2020. pp. 123259.
33. Azadi M, Ferdosi Heragh M, Bidi MA. Electrochemical characterizations of epoxy coatings embedded by modified calcium carbonate particles. In: Azadi M, editor. Progress in Color, Colorants, and Coatings. 1st edition. Tehran, Iran: Institute for Color Science and Technology; 2020. pp. 213–222.
34. Rehioui M, Abbout S, Benzidia B, Hammouch H, Erramli H, Ait Daoud N, Badrane N, Hajjaji N. Corrosion inhibiting effect of a green formulation based on Opuntia Dillenii seed oil for iron in acid rain solution. In: Rehioui M, editor. Heliyon. 1st edition. Amsterdam, Netherlands: Elsevier; 2021. pp. e06841.
35. Nataraja SE, Venkatesha TV, Tandon HC. Computational and experimental evaluation of the acid corrosion inhibition of steel by tacrine. In: Nataraja SE, editor. Corrosion Science. 1st edition. Amsterdam, Netherlands: Elsevier; 2012. pp. 214–223.
36. Liao B, Ma S, Zhang S, Li X, Quan R, Wan S, Guo X. Fructus cannabis protein extract powder as a green and high effective corrosion inhibitor for Q235 carbon steel in 1 M HCl solution. In: Liao B, editor. International Journal of Biological Macromolecules. 1st edition. Amsterdam, Netherlands: Elsevier; 2023. pp. 124358.
37. Wang Q, Zhang Q, Liu L, Zheng H, Wu X, Li Z, Gao P, Sun Y, Yan Z, Li X. Experimental, DFT, and MD evaluation of Nandina domestica Thunb. extract as green inhibitor for carbon steel corrosion in acidic medium. In: Wang Q, editor. Journal of Molecular Structure. 1st edition. Amsterdam, Netherlands: Elsevier; 2022. pp. 133367.

